



Variability of air-sea gas transfer velocities in the Baltic Sea

Nagel, Leila^a, Krall, Kerstin E.¹, and Jähne, Bernd^{1,2}

¹Institute of Environmental Physics, Heidelberg University, Im Neuenheimer Feld 229, 69120 Heidelberg, Germany

²Heidelberg Collaboratory for Image Processing, Heidelberg University, Berliner Straße 43, 69120 Heidelberg, Germany

^apreviously at: Institute of Environmental Physics, Heidelberg University, Im Neuenheimer Feld 229, 69120 Heidelberg, Germany

Correspondence: K. E. Krall

(Kerstin.Krall@iup.uni-heidelberg.de)

Abstract. Heat transfer velocities measured during three different campaigns in the Baltic Sea using the Active Controlled Flux Technique (ACFT) with wind speeds ranging from 5.3 to 14.8 m s⁻¹ are presented. Careful scaling of the heat transfer velocities to gas transfer velocities using Schmidt number exponents measured in a laboratory study allows to compare the measured transfer velocities to existing gas transfer velocity parameterizations, which use wind speed as the controlling parameter. The measured data and other field data clearly show that some gas transfer velocities are much lower than the empirical wind speed parameterizations. This indicates that the dependencies of the transfer velocity on the fetch, i. e., the history of the wind and the age of the wind wave field, and the effects of surface active material need to be taken into account.

1 Introduction

The transfer of a trace gas across the air sea interface is commonly characterized by the gas transfer velocity k , which links the gas flux j with the concentration difference across the interface, Δc ,

$$j = k\Delta c. \quad (1)$$

Traditionally, k is parameterized with the wind speed measured in 10 m height, u_{10} . Different authors proposed different functional dependencies between k and u_{10} , for example a gradual transition from a smooth to a wavy regime (Jähne, 1982), piecewise linear (Liss and Merlivat, 1986), linear and quadratic terms (Nightingale et al., 2000), quadratic (Wanninkhof, 1992) or cubic (Wanninkhof and McGillis, 1999).

In the last decades, the dual-tracer technique, especially with the tracer pair ³He/SF₆, has become state of the art of measuring the gas transfer velocity in situ. A recent review by Ho et al. (2011) proposed

$$k_{600} [\text{cm h}^{-1}] = 0.262 \pm 0.022 u_{10}^2 [u_{10} \text{ in m s}^{-1}] \quad (2)$$

as the best fit to all available ³He/SF₆ dual tracer data points.

However, mass balance techniques such as the dual tracer method have a large time constant of up to weeks and large spatial scales of a few tens of kilometers, smoothing away varying micrometeorological and surface conditions (e. g. the degree of surface contamination by surface active material).



In contrast, the eddy covariance method provides measurements of the gas transfer velocity on time scales below 1h and spatial scales of a few kilometers. However, bin averaging over wind speed intervals is frequently necessary, since even under idealized conditions, not all realizations of the turbulent field can be measured, so that each single flux measurement obtained during a 30 min time period is still uncertain (Garbe et al., 2014).

5 In this study, a thermographic technique is presented, which is capable of measuring the heat transfer velocity with a temporal resolution of about 20 minutes, which can then be scaled to gas transfer velocities. The active controlled flux technique was deployed during three cruises in the Baltic Sea to investigate the variability of the transfer velocities under field conditions.

2 Factors influencing air-sea gas exchange

10 A wealth of studies have shown, that, despite the common approach parameterizing the gas transfer velocity to wind speed alone, a multitude of other factors influence gas transfer, for example the contamination of the water surface with surface active material (e.g. Frew et al. (2004); Salter et al. (2011)), bubble entrainment (e.g. Woolf et al. (2007); Crosswell (2015)), fetch (e.g. Zhao et al. (2003); Woolf (2005)) and rain (e.g. Zappa et al. (2009); Harrison et al. (2012)).

15 Since the method discussed in this paper is insensitive to bubble contributions and can only be used to measure the interfacial part of the air sea gas transfer, and no measurements were performed in rain conditions, only the influence of surface active material and fetch will be discussed here.

2.1 Surfactants

20 One factor contributing to the disagreement between gas transfer velocities measured at the same wind speed are surface active materials (surfactants), which reduce the gas transfer velocity. This reduction in the gas transfer velocity in the presence of surfactants is not caused by the additional diffusion of the gas through the mono-molecular surfactant layer at the water surface (Frew et al., 1990), but by hydrodynamic effects in the mass boundary layer. Surfactant presence at the water surface inhibits eddy motion close to the surface and reduces fluid velocities. Upwelling at the surface is hindered by a reduction in the surface divergence due to the visco-elastic properties of the surfactant (McKenna and Bock, 2006). Vertical velocity fluctuations near the interface are considered vital to gas-transfer enhancement. Decreased vertical transport of fresh fluid towards the water surface results in a thicker boundary layer and thus a reduced transfer velocity (McKenna and McGillis, 2004).

25 Surfactants are enriched in the sea surface microlayer in the world's oceans (Wurl et al., 2011) over a wide range of wind speeds as high as $u_{10} = 13 \text{ m s}^{-1}$ (Sabbaghzadeh et al., 2017). In the Baltic sea, high surface activities were measured (Schmidt and Schneider, 2011), with a seasonal dependency in a near-shore position. The reduction of the gas transfer velocity due to surfactants has been observed in studies, where the gas transfer velocity was measured in laboratory setups in fresh water with added artificial surfactants (Mesarchaki et al., 2015; Krall, 2013; Lee and Saylor, 2010; Frew et al., 1995), in water sampled 30 from the ocean (Pereira et al., 2016; Schmidt and Schneider, 2011; Frew et al., 1990; Goldman et al., 1988), during field studies (Frew et al., 2004), as well as during field studies where artificial surfactants were released on the ocean surface (Salter et al.,



2011; Brockmann et al., 1982). Gas transfer is found to be highly variable, with a reduction of up to 60 % under surfactant influence.

The gas transfer velocity k of sparingly soluble gases is commonly parameterized with the friction velocity u_* , a measure for momentum input,

$$5 \quad k = \frac{1}{\beta} u_* S c^{-n} \quad (3)$$

with the momentum transfer resistance parameter β and the Schmidt number exponent n (Deacon, 1977; Jähne et al., 1979; Coantic, 1986; Jähne et al., 1989; Csanady, 1990). Both the momentum transfer resistance β and the Schmidt number exponent n depend on the hydrodynamic properties of the water surface. For a hydrodynamically smooth water surface, e.g. at very low wind speeds or under surfactant influence, the Schmidt number exponent is found to be $n = 2/3$, while for a wavy water surface, $n = 1/2$. For increasing friction velocity, this change from $n = 2/3$ to $n = 1/2$ is found to be smooth, rather than sudden (Jähne, 1987; Richter and Jähne, 2011). In addition, this change in the Schmidt number exponent depends also on the contamination of the water surface with surface active material, with the change starting at higher friction velocities and being steeper for a surfactant covered water surface (Krall, 2013).

2.2 Fetch and wave age

15 Another factor influencing the gas transfer velocity, which is disregarded in the widely used wind speed only parameterizations, is the dependency on fetch or the age of the wave field. Earliest indications that the fetch is an important parameter were seen by Broecker et al. (1978), who used an 18 m long wind-wave tank and found almost a doubling of the gas transfer velocity compared to the earlier work by Liss (1973), who used a tank of only 4.5 m length. Wanninkhof (1992) pointed out, that the differences observed between gas transfer measurements in lakes and the ocean might be caused by growing wave fields and thus increasing near surface turbulence over distances as high as a few hundreds of kilometers offshore. Zhao et al. (2003) and Woolf (2005) developed parameterization for the transfer velocity based the breaking-wave parameter (Toba and Koga, 1986) and the whitecap coverage, both of which depend on the fetch.

The considerations above indicate that there should be a dependency of the gas transfer velocity on the fetch. But unfortunately there is no solid knowledge because more detailed measurements and theories are lacking.

25 3 Measuring technique

3.1 Active thermography

The active controlled flux technique can be used to measure gas transfer velocities under laboratory as well as under field conditions with a high temporal (minutes) and spatial (meters) resolution, using heat as a proxy tracer. A carbon dioxide laser with an scanning optic is used to deposit energy directly to the water surface. An infrared camera measures the resulting heating.



For this study the system theory approach proposed in Jähne et al. (1989) was used. In this approach, the laser is switched on and off with changing frequencies. At low laser forcing frequencies the water surface will reach the thermal equilibrium, resulting in a constant heating. At higher forcing frequencies this equilibrium is not reached and the measured amplitude is damped. Using Fourier analysis to determine this amplitude damping in dependency of the laser forcing frequency, the time to reach the thermal equilibrium, which corresponds to the response time of the system, is calculated. It is linked to the transfer velocity by (Jähne et al. (1987))

$$k_{\text{heat}} = \sqrt{\frac{D_{\text{heat}}}{\tau}} \quad \text{or} \quad \tau = \frac{D_{\text{heat}}}{k_{\text{heat}}^2}. \quad (4)$$

This analysis technique is particularly suitable for field measurements as it requires no absolute calibration. A more detailed description of the analysis method, the necessary correction for the penetration depth of the infrared camera and the error estimation can be found in Nagel (2014).

3.2 Scaling heat transfer velocities to gas transfer velocities

To compare the measured transfer velocities of heat to the transfer velocities of a gas like CO₂, Schmidt number scaling is applied,

$$k_{\text{gas}} = k_{\text{heat}} \left(\frac{\text{Sc}}{\text{Pr}} \right)^{-n}, \quad (5)$$

where k_{gas} and k_{heat} are the transfer velocities for the gas and heat, respectively. The Schmidt number $\text{Sc} = \nu/D_{\text{gas}}$ and the Prandtl number $\text{Pr} = \nu/D_{\text{heat}}$ are given by the kinematic viscosity of the water divided by the diffusion coefficient of the gas and of heat in water, respectively. The Schmidt number exponent n varies between $n = 2/3$ for a flat and $n = 1/2$ for a wavy water surface (Jähne and Haußecker (1998), Richter and Jähne (2011), Krall (2013)).

However, using heat as a proxy for a gas tracer has one significant drawback. Diffusion of heat is about one hundred times faster than diffusion of a dissolved gas in water. Because of this, any uncertainty in the Schmidt number exponent n leads to a relative large uncertainty for the heat transfer velocity scaled to a gas transfer velocity. It is generally given by

$$\frac{\Delta k}{k_{\text{gas}}} = \ln \left(\frac{\text{Sc}}{\text{Pr}} \right) \Delta n. \quad (6)$$

where Δk and Δn are the absolute uncertainties for the transfer velocity and the Schmidt number exponent, respectively. For the whole expected range of $n = 2/3$ to $1/2$, $\Delta n = \pm 0.083$ (Fig. 1) and $\text{Sc}/\text{Pr} \approx 600/9$, the relative scaling error is $\pm 35\%$. This is quite a large uncertainty.

In the past decade, several studies (Asher et al., 2004; Atmane et al., 2004; Zappa et al., 2004; Jessup et al., 2009) found deviations between the Schmidt number scaled heat and the simultaneously measured gas transfer velocities. However, a more recent study by Nagel et al. (2015) showed that using a model independent analysis method, as proposed by Jähne et al. (1989) and the correct Schmidt number exponent results in a good agreement.

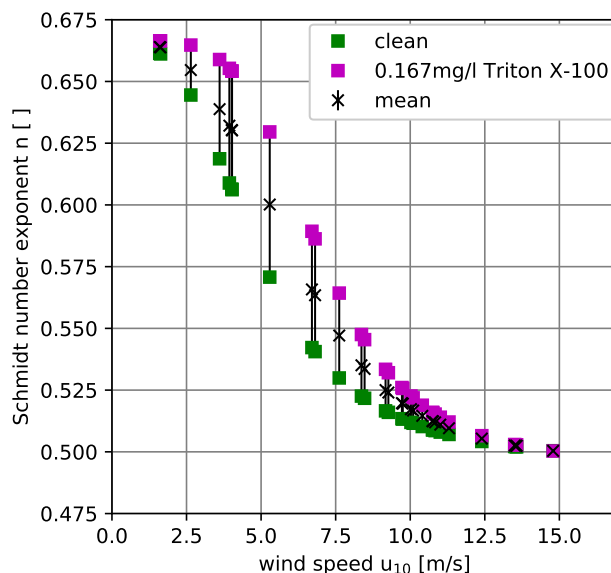


Figure 1. Possible ranges of Schmidt number exponents for a clean and surfactant covered water surface as a function of the wind speed as inferred from experiments in the Heidelberg *Aeolotron* wind-wave tank (Krall, 2013) for the wind speeds encountered during this study. Friction velocities measured in the *Aeolotron* were taken from Bopp (2011) and converted to the wind speed in 10 m height using the drag coefficient parameterization by Edson et al. (2013). To scale the heat transfer velocities measured in the present work, the mean values of the Schmidt number exponent were used.

For field measurements, the importance of using a Schmidt number exponent depending on the water surface condition is also highlighted in Esters et al. (2017), who relate the gas transfer velocity to the turbulent energy dissipation rate.

Currently, there are no measurement techniques available to measure the Schmidt number exponent in the field with the same temporal resolution as the heat transfer measurements. Therefore, the scaling in the present work was done using Schmidt number exponents measured in the Heidelberg *Aeolotron* wind wave tank, see 1 (Krall, 2013), as opposed to Schimpf et al. (2011), who used a fixed Schmidt number exponent of $1/2$. (Jähne et al. (1987), Richter and Jähne (2011), Krall (2013)). In Krall (2013), Schmidt number exponents were measured with different concentrations of the surface active material (surfactant) *Triton X-100*. The mean of the Schmidt number exponent of the two extreme cases presented in Krall (2013), corresponding to clean water and water with $167 \mu\text{g l}^{-1}$ Triton X-100, respectively, was used to scale the heat transfer velocities to gas transfer velocities to account for possible contamination of the water surface with surface active material. The difference between the mean and both extreme values of the Schmidt number exponent was used as the uncertainty of the Schmidt number exponent. Since the *Aeolotron* wind-wave tank is an annular facility, it has virtually unlimited fetch, comparable with open ocean conditions.



Due to the lack of simultaneously measured Schmidt number exponents in the field, this approach is more realistic than using $n = 1/2$ for all encountered wind conditions disregarding a potentially smooth condition ($n = 2/3$) of the water surface. The approach used here reduces the uncertainty of Δn from ± 0.083 to $< \pm 0.030$ (Fig. 1). The resulting relative uncertainty of k is then $\Delta k/k < \pm 13\%$.

- 5 Another source of uncertainty lies in transferring the lab measurements of the Schmidt number exponent to the field conditions, since in the lab, the friction velocity u_* is measured (Bopp, 2011) as opposed to the wind speed in 10 m height which is commonly measured in the field. To convert lab measurements to field conditions, the drag coefficient, $C_D = u_*^2/u_{10}^2$ taken from Edson et al. (2013) was used.

4 Measurements

10 4.1 Experimental setup on ship

To use the CFT method described in Sec. 3.1, a CO₂-Laser (Firestar f200, Synrad, Inc.) was used to heat the water surface. A scanning system (Micro Max 671, Cambridge Technology, Inc.) was used to widen the laser to create a heated patch on the water surface. The temperature response of the water surface was recorded with an infrared camera (CMT 256, Thermosensorik). Laser, scanner and camera are synchronised by custom electronics. A water tight box, including the IR laser, the IR camera
15 and the electronics was installed on rails on top of an aluminum cradle at the bow of the research vessels. During transit times the box was retracted and fixed over the vessel, while it was moved over the ocean during measurement times. A more detailed description of all used instruments is given in Nagel (2014).

Measurements were only conducted at stations, where the vessel was standing at one position. Nevertheless due to currents the water surface moved relative to the ship. As direct sun irradiation disturbs the infrared signals, most measurement were
20 conducted during night time or on cloudy days. Nevertheless, reflections of thermal signature of the sky and the ship itself can not be avoided. However, the periodic forcing of the heat flux as described in Sect. 3.1, suppresses these effects (lock-in technique).

Wind speed measured in 10 m height was provided by each vessels weather station. On FS *Alkor*, one minute mean wind speeds were stored only for the times during which measurements with the ACFT were performed. On RV *Aranda*, ten second
25 mean values were stored for the whole duration of the cruise. During data processing, averages of the stored values were calculated for the times during which the respective ACFT measurements were performed.

4.2 Baltic Sea campaigns 2009 and 2010

Three ship campaigns were conducted in 2009 and 2010.

Figure 2 show the tracks of these three cruises. The first one (Alkor Cruise 336, Schmidt (2009)) took place from 25 April
30 2009 until 7 March 2009 on the German research vessel FS *Alkor*. It included measurements north-west of Rügen and the Gotland Sea. The second cruise on the same vessel (Alkor Cruise 356, Schneider (2010)), between 30 June and 13 July 2010

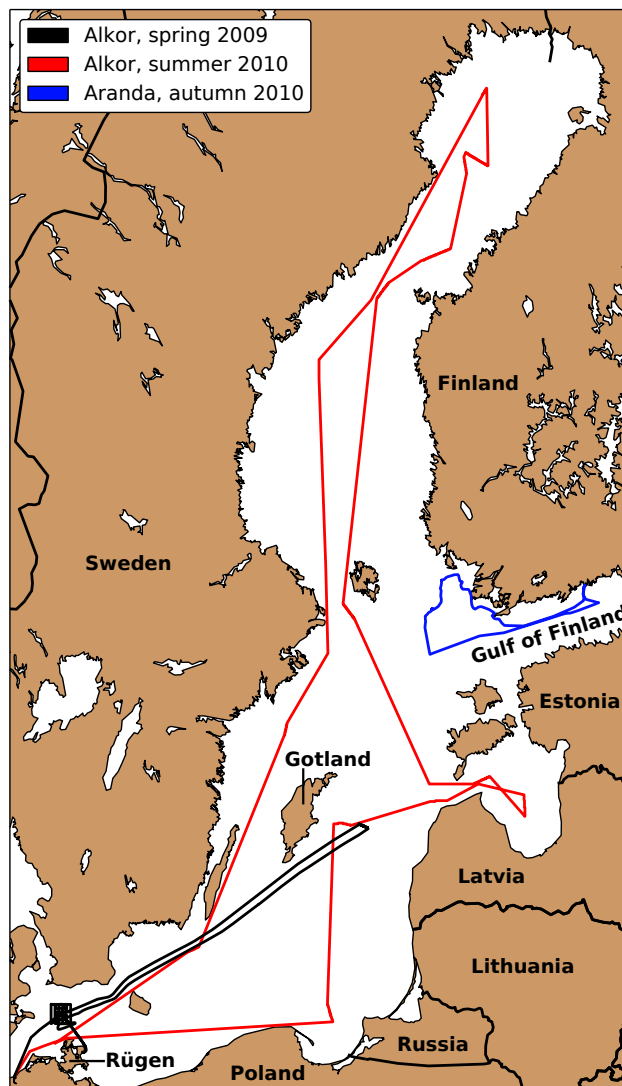


Figure 2. Map of the Baltic Sea. The tracks of the three cruises are shown.

included measurement stations spread over the whole Baltic Sea. The third cruise took place on the Finnish research vessel RV *Aranda* from 14 September until 19 September 2010. Due to the stormy weather conditions, most measurements were conducted in the Finnish archipelago and only two measurements were conducted under open ocean conditions in the Gulf of Finland.

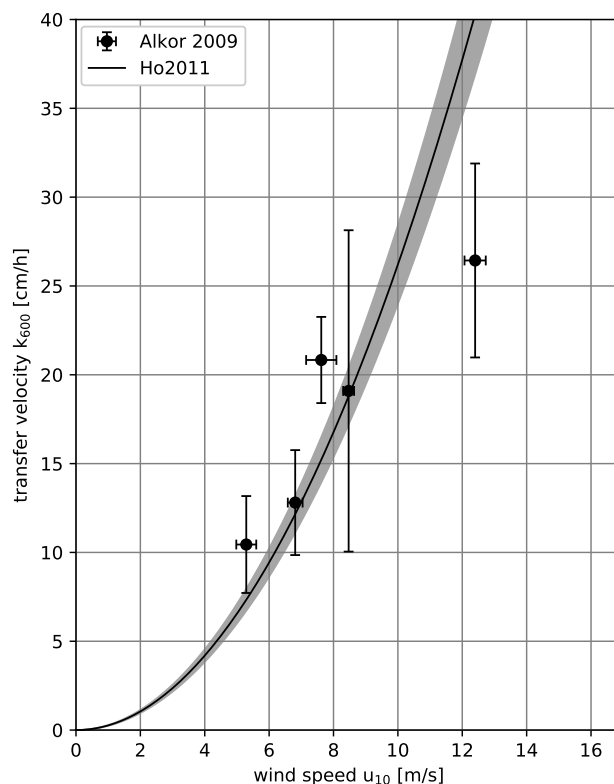


Figure 3. Measured k_{600} transfer velocities plotted against the wind speed of the FS *Alkor* Spring 2009 cruise. For comparison the best fit of Ho et al. (2011), Eq. 2 is added.

5 Results

5.1 Measured transfer velocities

First results of the cruise in 2009 are already published in Schimpf et al. (2011). For this study a re-evaluation with slight differences in the correction of the penetration depth of the infrared camera was done. Also, the improved Schmidt number scaling described in section 3.2 was used, while Schimpf et al. (2011) used $n=1/2$ for all conditions. The obtained heat transfer velocities are given in Tab. A1. Figure 3 shows the measured transfer velocities, scaled to a Schmidt number of 600. To compare the results with other field measurements the parameterization by Ho et al. (2011), which parameterizes the transfer velocity with the wind speed is also shown.

Figure 4 shows the measured heat transfer velocities over the wind speed in comparison to the same parameterization as used for the measurements in 2009. Schmidt number scaling was done with the same method as for the *Alkor* 2009 data set. During most of the FS *Alkor* campaign in 2010 the wind speeds were rather low. At low wind speeds, the response time of

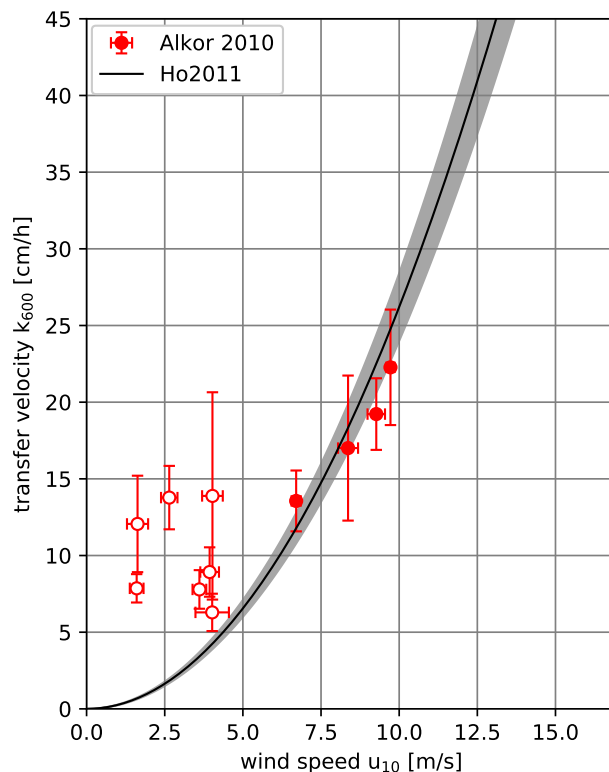


Figure 4. Measured k_{600} transfer velocities plotted against the wind speed of the FS *Alkor* Summer 2010 cruise. Conditions, for which the measured transfer velocity is likely overestimated are marked with open circles and will not be used for further analysis. For comparison the wind speed parameterization taken from Ho et al. (2011) is added.

the system is very high, as it decreases with the square of the transfer velocity (Eq. 4). The time a water parcel stays in the heated patch (residence time) is limited due to surface currents and the movement of the ship relatively to the water surface. To be able to reach the thermal equilibrium, the residence time has to be longer than the response time of the water surface. Otherwise a lower temperature and therefore a higher amplitude damping will be observed, which leads to an overestimation of the measured transfer velocities. The residence times were estimated from the infrared images themselves by measuring the time a single structure stayed in the heated patch. All measurements with wind speeds of 4 ms^{-1} and below are not reliable, because the estimated residence times were found to be too long. Therefore they will be excluded from further analysis.

This highlights the difficulties of measuring gas transfer velocities at very low wind speeds. However, difficulties also exist with other approaches to measure the gas transfer velocity in the field, such as dual tracer studies, where the time scales required for measurements are very long at low wind speeds, and sufficiently long periods of low winds are rarely encountered.

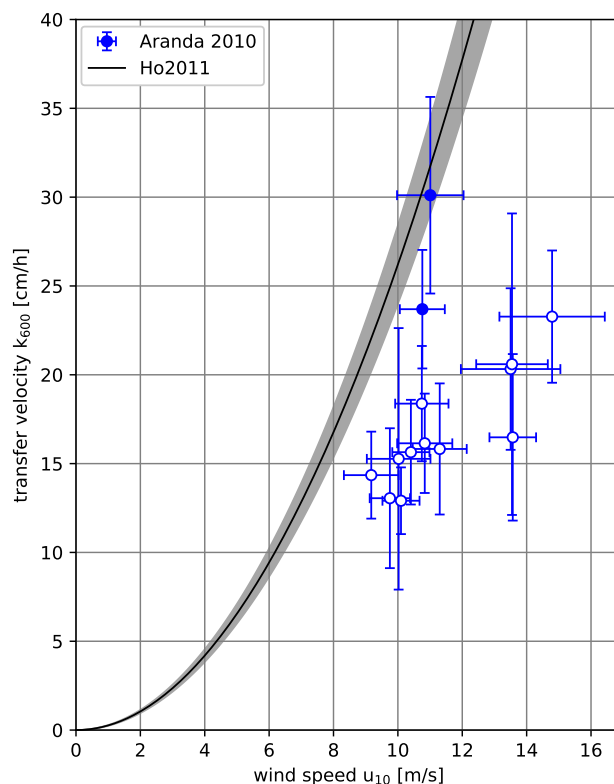


Figure 5. Measured k_{600} transfer velocities plotted against the wind speed of the RV *Aranda* Fall 2010 cruise. The filled circles show the open ocean measurements, while the open circles are data from the archipelago. For comparison, the wind speed parameterization by Ho et al. (2011) is also shown.

The heat transfer velocities scaled to $Sc=600$ measured on RV *Aranda* in 2010 are shown in Fig. 5. The transfer velocities measured in the shielded archipelago are significantly lower than the ones measured under open ocean conditions.

5.2 Comparison with other field and laboratory data

Fig. 6 shows a comparison between the measured transfer velocities with the empirical parameterization of Ho et al. (2011).

- 5 The measurements from the *Alkor* 2009 and *Alkor* 2010 cruises coincide within the error margins with the empirical parameterization by Ho, except for the value at the highest wind speed, which is approx. 40% lower. The two open ocean measurements during the RV *Aranda* cruise 2010 are slightly lower than the empirical parameterization, but still close to it.

This is, however, not the case for the RV *Aranda* cruise measurements in the shielded archipelago. The measured values are significantly lower. On average, the values are only about one half of the transfer velocities predicted by the empirical

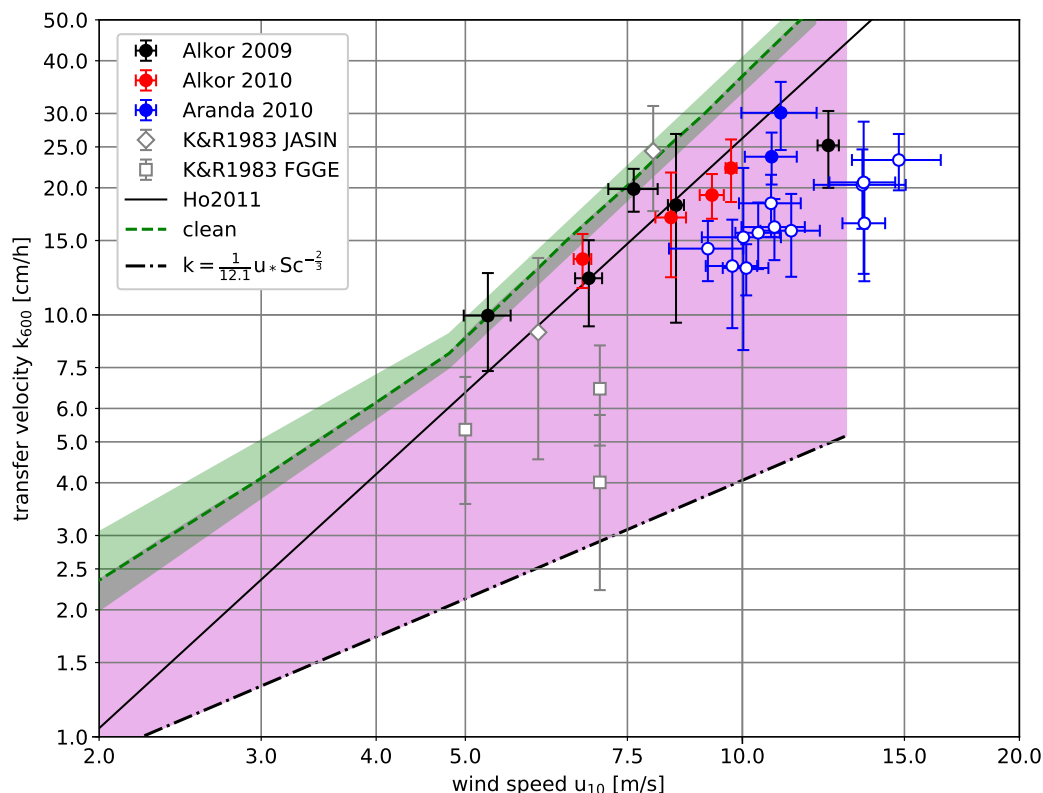


Figure 6. Comparison of scaled heat transfer velocities measured in the Baltic Sea and gas transfer velocities measured in the Heidelberg *Aeolotron* wind-wave facility with a clean water surface (green shaded area). For the measurements on RV *Aranda* in 2010 open ocean conditions, assumed to be with a virtually unlimited fetch, are marked with filled circles, while the fetch limited measurements in the archipelago are marked with open circles. Also shown is the lower limit for a smooth water surface, Eq. 3. The region between the transfer velocities measured with a clean water surface as the upper boundary and the values for a smooth water surface as the lower boundary for possible transfer velocities is shaded in magenta. Also shown are the data set of Kromer and Roether (1983) (K&R1983) and the parameterization by Ho et al. (2011).

parameterization. Because no other information is available, it is impossible to distinguish whether this is caused by the limited fetch or by surfactants or by a combination of both.

A very helpful hint comes, however, from an old data set which constitutes the most diligently measured gas transfer velocities using the Radon deficit method (Kromer and Roether, 1983; Roether and Kromer, 1984). One part of this data set was measured during the JASIN cruise in the North Atlantic with highly varying wind speeds. The measured gas transfer velocities are higher or as high as predicted by the empirical parameterization. However, the transfer velocities measured during the FGGE cruise with constantly blowing trade winds are significantly lower. One value is three times lower than predicted by the



empirical parameterization. These measurements clearly indicate that even at the open ocean (i. e. without fetch limitations) there will be significant differences in the gas transfer velocity. The data suggests that this effect may be as large as a factor of five.

It is obvious that the deviations between the measurements shown here and the H_o parameterization cannot be explained by
5 fetch or the age of the wave field alone, because both at a young wind wave field in the shielded archipelago and at very old
wind wave fields (FGGE), significant reductions in the gas transfer velocities are observed.

At this point it is helpful, to compare the field data with laboratory data. A direct comparison is not useful, because the
conditions concerning the wave field and surface contamination will be different. But laboratory data are very helpful to explore
the upper and lower limits of the gas transfer velocity at a given wind speed. For the comparison, we used gas transfer velocities
10 measured in the Heidelberg *Aeolotron*. This is an annular facility with virtually unlimited fetch and thus may resemble the ocean
conditions in the best possible way. Those gas transfer velocities were measured with the method described in Mesarchaki et al.
(2015) and are published in Krall (2013).

The gas transfer velocities measured when the water surface in the *Aeolotron* was carefully cleaned by skimming the top
layer of the water before the start of each measurement to remove surface active material, can be considered to be the upper
15 limit (green shaded area in Fig. 6).

The lower limit is constituted by the gas transfer velocities predicted by Deacon (1977) (eqn. 3 with $n=2/3$ and $\beta = 12.1$) for
a smooth water surface. These values have been confirmed by measurements in a small annular wind/wave facility when the
water surface was covered by surfactants (Jähne et al., 1979). The highest friction velocity in water at which the water surface
remained smooth and without wind waves in this facility was 1.4 cm/s corresponding to a smooth water surface up to a wind
20 speed of $u_{10} \approx 13$ m/s. This is supported by the findings of Sabbaghzadeh et al. (2017), who measured surfactant enrichment
in the sea surface microlayer up to $u_{10} \approx 13$ m/s as well.

The region between these upper and lower bounds for gas transfer is shaded in a magenta color in Fig. 6. This difference
between highest and lowest possible gas transfer velocities alone indicates that the gas transfer is highly variable and not only
dependent on wind speed alone. All shown field data as well as the H_o parameterization are compatible with this shaded region
25 of possible gas transfer rates.

6 Conclusions and outlook

Heat exchange measurements were conducted in the Baltic Sea during three different campaigns using the active controlled flux
technique. The measured heat transfer velocities, scaled to gas transfer velocities using realistic Schmidt number exponents,
show high variability even at the same wind speed. New is that even at high wind speeds in the range of 8 to 15 m/s significantly
30 lower gas transfer velocities were measured, which were about a factor of two lower than the average transfer velocities
measured by the dual tracer technique and parameterized by the relation of Ho et al. (2011). Based on the field data alone it is
not possible to distinguish fetch effects from effects by surface films.



This study clearly indicates that a better understanding of air-sea gas transfer requires more systematic measurements of the effects of fetch (or the age of the wave field) and surfactants. In the field the most promising approach is eddy covariance measurements together with active thermography.

For laboratory measurements some serious limitations must be overcome. One is the fetch gap. In linear facilities only very short fetches can be studied, which are no longer than the maximum length of the water tunnel in the facility. Even at these short fetches, significant variations of the gas transfer rate can be measured. This has recently been demonstrated by Kunz and Jähne (2018) using active thermography.

In order to increase the fetch range available in the lab, gas exchange measurements could be performed in annular facilities under unsteady wind speed conditions. In the Heidelberg *Aeolotron* it is possible to switch on the wind in a few seconds, while it takes several minutes for the wave field to develop to a stationary state. Unfortunately, it is very hard to make gas exchange measurements with a temporal resolution of below a minute using conventional mass balance techniques.

A very promising technique for fast measurements of gas transfer is the recently developed mass boundary layer imaging technique (Kräuter et al., 2014; Kräuter, 2015). Using this technique will enable the measurement of the gas transfer velocity simultaneously and in the same footprint as the heat transfer velocity. This will allow a direct comparison as well as in-depth studies of the physical mechanisms governing air-sea gas and heat transfer.

Appendix A: Numerical values of the measured transfer velocities

Tables A1, A2 and A3 give the numerical values of the measurements conducted during the cruises in the Baltic Sea.

Table A1. Measured heat transfer velocities k_{heat} in dependency of time, position, wind speed and water and air temperature for the measurements on FS *Alkor* in 2009. Furthermore the Prandtl number Pr , the Schmidt number exponent n and the scaled transfer velocity k_{600} are given. The given times are approximate starting times in UTC. Each measurement lasted about 20 min.

number	date yyyy/mm/dd	time hh:mm	position		u_{10} [m/s]	T_{water} [°C]	T_{air} [°C]	k_{heat} [cm/h]	Pr	n	k_{600} [cm/h]
			N	E							
A1	2009/04/28	19:55	55.002	13.169	8.47 ± 0.17	7.3	10.8	158.6 ± 74.8	10.38	0.534 ± 0.012	18.2 ± 8.6
A2	2009/04/30	02:30	55.122	13.103	12.4 ± 0.33	7.4	8.2	195.9 ± 40.4	10.38	0.505 ± 0.001	25.2 ± 5.2
A3	2009/05/01	20:05	56.389	17.591	5.29 ± 0.31	5.7	6.4	109.8 ± 25.6	11.0	0.6 ± 0.029	10.0 ± 2.6
A4	2009/05/02	20:20	57.337	20.016	6.81 ± 0.23	6.2	8.0	117.3 ± 24.8	10.81	0.563 ± 0.023	12.2 ± 2.8
A5	2009/05/03	20:45	57.366	19.904	7.62 ± 0.47	6.5	7.9	179.8 ± 16.8	10.7	0.547 ± 0.017	19.9 ± 2.3



Table A2. Measured heat transfer velocities k_{heat} in dependency of time, position, wind speed and water and air temperature for the measurements on FS *Alkor* in 2010. Furthermore the Prandtl number Pr, the Schmidt number exponent n and the scaled transfer velocity k_{600} are given. The given times are approximate starting times in UTC. Each measurements lasted about 20 min.

number	date yyyy/mm/dd	time hh:mm	position		u_{10} [m/s]	T_{water} [°C]	T_{air} [°C]	k_{heat} [cm/h]	Pr	n	k_{600} [cm/h]
			N	E							
B1	2010/07/02	00:05	54.951	19.233	4.0±0.3	17.0	15.8	217.4±103.3	7.63	0.63±0.024	13.9±6.8
B2	2010/07/02	00:35	55.064	19.175	3.9±0.3	16.6	15.8	139.6±20.9	7.74	0.632±0.023	8.9±1.6
B3	2010/07/03	06:05	57.383	19.490	1.6±0.2	17.9	17.7	146.9±17.2	7.3	0.664±0.003	7.9±0.9
B4	2010/07/03	23:05	57.658	21.653	3.6±0.2	18.4	18.5	130.2±17.6	7.3	0.639±0.02	7.8±1.3
B5	2010/07/04	22:05	57.903	22.594	4.0±0.5	19.5	20.1	103.2±16.7	7.09	0.63±0.024	6.3±1.2
B6	2010/07/05	20:30	59.857	19.643	6.7±0.1	15.2	16.4	154.9±16.3	8.1	0.566±0.024	13.6±2.0
B7	2010/07/08	18:50	65.215	22.638	8.4±0.3	14.5	16.2	168.7±46.1	8.23	0.535±0.012	17.0±4.7
B8	2010/07/10	22:35	58.561	18.244	2.6±0.3	18.9	20.9	249.4±35.7	7.19	0.655±0.01	13.8±2.1
B9	2010/07/10	23:05	58.567	18.246	1.6±0.3	18.9	20.4	227.3±59.2	7.19	0.664±0.003	12.1±3.1
B10	2010/07/11	19:15	58.567	16.240	9.7±0.1	19.6	22.5	225.3±37.6	6.99	0.52±0.006	22.3±3.8
B11	2010/07/11	19:45	58.847	16.206	9.3±0.3	19.9	22.4	198.2±23.0	6.99	0.524±0.008	19.2±2.3



Table A3. Measured heat transfer velocities k_{heat} in dependency of time, position, wind speed and water and air temperature for the measurements on RV *Aranda* in 2010. Furthermore the Prandtl number Pr , the Schmidt number exponent n and the scaled transfer velocity k_{600} are given. The given times are approximate starting times in UTC. Each measurements lasted about 20 min. All measurements were conducted in a fetch-limited position with the exception of the two conditions marked with an asterisk (*).

number	date yyyy/mm/dd	time hh:mm	position		u_{10} [m/s]	T_{water} [°C]	T_{air} [°C]	k_{heat} [cm/h]	Pr	n	k_{600} [cm/h]
			N	E							
C1	2010/09/15	18:05	59.899	21.502	10.4±0.6	14.9	13.3	143.6±25.7	8.07	0.515±0.004	15.6±2.8
C2	2010/09/15	21:25	59.899	21.502	9.2±0.8	14.8	13.8	137.6±21.8	8.1	0.525±0.008	14.4±2.3
C3	2010/09/16	04:15	59.899	21.502	13.6±0.7	14.9	14.1	143.6±38.9	8.07	0.502±0.0	16.5±4.5
C4	2010/09/16	05:30	59.899	21.502	14.8±1.6	14.9	14.0	201.0±30.7	8.07	0.5±0.0	23.3±3.5
C5	2010/09/16	16:10	59.899	21.502	13.5±1.5	14.9	13.9	177.2±37.8	8.07	0.503±0.0	20.3±4.3
C6	2010/09/16	17:15	59.899	21.502	13.5±1.1	14.9	13.7	179.5±70.5	8.07	0.502±0.0	20.6±8.1
C7	2010/09/16	20:55	59.893	21.486	10.0±1.0	14.8	13.6	141.6±65.0	8.1	0.517±0.005	15.3±7.0
C8	2010/09/16	21:50	59.893	21.486	10.1±0.6	14.7	14.0	119.2±16.3	8.12	0.517±0.005	12.9±1.8
C9	2010/09/17	04:15	59.893	21.486	10.7±0.8	14.5	13.7	166.2±27.9	8.17	0.512±0.004	18.4±3.1
C10	2010/09/17	05:25	59.893	21.486	10.8±0.9	14.6	13.7	145.9±24.0	8.14	0.512±0.003	16.1±2.7
C11	2010/09/17	16:15	59.893	21.486	11.3±0.8	14.6	13.4	141.5±31.4	8.14	0.51±0.003	15.8±3.5
C12	2010/09/17	19:15	59.893	21.486	9.8±0.6	14.5	13.6	121.6±34.8	8.17	0.519±0.006	13.1±3.8
C13*	2010/09/18	13:05	59.378	21.441	11.0±1.0	14.0	12.2	268.5±49.2	8.29	0.511±0.003	30.1±5.5
C14*	2010/09/18	13:35	59.378	21.441	10.8±0.7	13.2	11.3	209.9±29.4	8.49	0.512±0.004	23.7±3.3



Competing interests. None.

Acknowledgements. We would like to thank Prof. Dr. Kimmo Kahma and Dr. Heidi Pettersson, Finish Meteorological Institute for the possibility to participate in the Aranda CO₂_WAVE10_CTD10/2010 cruise. We would also like to thank Dr. Robert Schmidt and Dr. Bernd Schneider, Institut für Ostseeforschung, Warnemünde for the chief scientist work during the cruises *Alkor* 336 and *Alkor* 356. We are grateful
5 for the assistance onboard by the captains and crews of RV *Aranda* and FS *Alkor*. We would like to thank Dr. Uwe Schimpf and Dr. Günther Balschbach for help with preparing and conducting the measurements as well as logistical support. Financial support for this work by the German Federal Ministry of Education and Research (BMBF) joint project "Surface Ocean Processes in the Anthropocene" (SOPRAN, FKZ 03F0462F, 03F0611F and 03F0622F) within the international SOLAS project is gratefully acknowledged.



References

- Asher, W. E., Jessup, A. T., and Atmane, M. A.: Oceanic application of the active controlled flux technique for measuring air-sea transfer velocities of heat and gases, *J. Geophys. Res.*, 109, C08S12, <https://doi.org/10.1029/2003JC001862>, 2004.
- Atmane, M. A., Asher, W., and Jessup, A. T.: On the use of the active infrared technique to infer heat and gas transfer velocities at the air-water free surface, *J. Geophys. Res.*, 109, C08S14, <https://doi.org/10.1029/2003JC001805>, 2004.
- 5 Bopp, M.: Messung der Schubspannungsgeschwindigkeit am Heidelberger Aeolotron mittels der Impulsbilanzmethode, Bachelor thesis, Institut für Umweltphysik, Fakultät für Physik und Astronomie, Univ. Heidelberg, 2011.
- Brockmann, U. H., Hühnerfuss, H., Kattner, G., Broecker, H.-C., and Hentzschel, G.: Artificial surface films in the sea area near Sylt, *Limnology and Oceanography*, 27, 1050–1058, <https://doi.org/10.4319/lo.1982.27.6.1050>, <http://dx.doi.org/10.4319/lo.1982.27.6.1050>,
10 1982.
- Broecker, H. C., Siems, W., and Petermann, J.: The influence of wind on CO₂ exchange in a wind wave tunnel, including the effects of monolayers, *J. Marine Res.*, 36, 595–610, 1978.
- Coantic, M.: A model of gas transfer across air–water interfaces with capillary waves, *J. Geophys. Res.*, 91, 3925–3943, <https://doi.org/10.1029/JC091iC03p03925>, 1986.
- 15 Crosswell, J. R.: Bubble Clouds in Coastal Waters and Their Role in Air-Water Gas Exchange of CO₂, *Journal of Marine Science and Engineering*, 3, 866–890, <https://doi.org/10.3390/jmse3030866>, <http://www.mdpi.com/2077-1312/3/3/866>, 2015.
- Csanady, G. T.: The role of breaking wavelets in air-sea gas transfer, *J. Geophys. Res.*, 95, 749–759, <https://doi.org/10.1029/JC095iC01p00749>, 1990.
- Deacon, E. L.: Gas transfer to and across an air-water interface, *Tellus*, 29, 363–374, <https://doi.org/10.3402/tellusa.v29i4.11368>, 1977.
- 20 Edson, J. B., Jampana, V., Weller, R. A., Bigorre, S. P., Plueddemann, A. J., Fairall, C. W., Miller, S. D., Mahrt, L., Vickers, D., and Hersbach, H.: On the exchange of momentum over the open ocean, *J. Phys. Oceanogr.*, 43, 1589–1610, <https://doi.org/10.1175/JPO-D-12-0173.1>, 2013.
- Esters, L., Landwehr, S., Sutherland, G., Bell, T. G., Christensen, K. H., Saltzman, E. S., Miller, S. D., and Ward, B.: Parameterizing air-sea gas transfer velocity with dissipation, *J. Geophys. Res.*, 122, 3041–3056, <https://doi.org/10.1002/2016JC012088>, 2017.
- 25 Frew, N., Bock, E., Schimpf, U., Hara, T., Haussecker, H., Edson, J., McGillis, W., Nelson, R., McKenna, S., Uz, B., and Jähne, B.: Air-sea gas transfer: Its dependence on wind stress, small-scale roughness, and surface films, *J. Geophys. Res.*, 109, C08S17, <https://doi.org/10.1029/2003JC002131>, 2004.
- Frew, N. M., Goldman, J. C., Denett, M. R., and Johnson, A. S.: Impact of phytoplankton-generated surfactants on air-sea gas-exchange, *J. Geophys. Res.*, 95, 3337–3352, <https://doi.org/10.1029/JC095iC03p03337>, 1990.
- 30 Frew, N. M., Bock, E. J., McGillis, W. R., Karachintsev, A. V., Hara, T., Münsterer, T., and Jähne, B.: Variation of air–water gas transfer with wind stress and surface viscoelasticity, in: *Air-water Gas Transfer, Selected Papers from the Third International Symposium on Air-Water Gas Transfer*, edited by Jähne, B. and Monahan, E. C., pp. 529–541, AEON, Hanau, <https://doi.org/10.5281/zenodo.10405>, 1995.
- Garbe, C. S., Rutgersson, A., Boutin, J., Delille, B., Fairall, C. W., Gruber, N., Hare, J., Ho, D., Johnson, M., de Leeuw, G., Nightingale, P., Pettersson, H., Piskozub, J., Sahlee, E., Tsai, W., Ward, B., Woolf, D. K., and Zappa, C.: Transfer across the air-sea interface, in: *Ocean-Atmosphere Interactions of Gases and Particles*, edited by Liss, P. S. and Johnson, M. T., pp. 55–112, Springer, https://doi.org/10.1007/978-3-642-25643-1_2, 2014.



- Goldman, J. C., Dennet, M. R., and Frew, N. M.: Surfactant effects on air-sea gas exchange under turbulent conditions, *Deep Sea Research*, 35, 1953–1970, [https://doi.org/10.1016/0198-0149\(88\)90119-7](https://doi.org/10.1016/0198-0149(88)90119-7), 1988.
- Harrison, E. L., Veron, F., Ho, D. T., Reid, M. C., Eggleston, S. S., Orton, P., and McGillis, W. R.: Nonlinear interaction between rain and wind induced air-water gas exchange, *J. Geophys. Res.*, 117, <https://doi.org/10.1029/2011JC007693>, in Prep, 2012.
- 5 Ho, D. T., Wanninkhof, R., Schlosser, P., Ullman, D. S., Hebert, D., and Sullivan, K. F.: Toward a universal relationship between wind speed and gas exchange: Gas transfer velocities measured with $^3\text{He}/\text{SF}_6$ during the Southern Ocean Gas Exchange Experiment, *J. Geophys. Res.*, 116, C00F04, <https://doi.org/10.1029/2010JC006854>, 2011.
- Jessup, A. T., Asher, W. E., Atmane, M., Phadnis, K., Zappa, C. J., and Loewen, M. R.: Evidence for complete and partial surface renewal at an air-water interface, *Geophys. Res. Lett.*, 36, 1–5, <https://doi.org/10.1029/2009GL038986>, 2009.
- 10 Jähne, B.: Trockene Deposition von Gasen über Wasser (Gasaustausch), in: Austausch von Luftverunreinigungen an der Grenzfläche Atmosphäre/Erdoberfläche, Zwischenbericht für das Umweltbundesamt zum Teilprojekt 1: Deposition von Gasen, BleV-R-64.284-2, edited by Flothmann, D., Battelle Institut, Frankfurt, <https://doi.org/10.5281/zenodo.10278>, 1982.
- Jähne, B.: Image sequence analysis of complex physical objects: nonlinear small scale water surface waves, in: Proc. of 1st International Conference on Computer Vision, pp. 191–200, IEEE, London, UK, <https://doi.org/10.5281/zenodo.13126>, 1987.
- 15 Jähne, B. and Haußecker, H.: Air-water gas exchange, *Annu. Rev. Fluid Mech.*, 30, 443–468, <https://doi.org/10.1146/annurev.fluid.30.1.443>, 1998.
- Jähne, B., Münnich, K. O., and Siegenthaler, U.: Measurements of gas exchange and momentum transfer in a circular wind-water tunnel, *Tellus*, 31, 321–329, <https://doi.org/10.1111/j.2153-3490.1979.tb00911.x>, 1979.
- Jähne, B., Münnich, K. O., Bössinger, R., Dutzi, A., Huber, W., and Libner, P.: On the parameters influencing air-water gas exchange, *J. Geophys. Res.*, 92, 1937–1950, <https://doi.org/10.1029/JC092iC02p01937>, 1987.
- Jähne, B., Libner, P., Fischer, R., Billen, T., and Plate, E. J.: Investigating the transfer process across the free aqueous boundary layer by the controlled flux method, *Tellus*, 41B, 177–195, <https://doi.org/10.3402/tellusb.v41i2.15068>, 1989.
- Krall, K. E.: Laboratory Investigations of Air-Sea Gas Transfer under a Wide Range of Water Surface Conditions, Dissertation, Institut für Umweltphysik, Fakultät für Physik und Astronomie, Univ. Heidelberg, <https://doi.org/10.11588/heidok.00014392>, 2013.
- 25 Kromer, B. and Roether, W.: Field measurements of air-sea gas exchange by the radon deficit method during JASIN 1978 and FGGE 1979, *Meteor. Forschungsergebnisse, Deutsche Forschungsgemeinschaft, Reihe A/B*, 24, 55–76, <https://doi.org/10.1594/PANGAEA.604844>, 1983.
- Kräuter, C.: Visualization of air-water gas exchange, Dissertation, Institut für Umweltphysik, Fakultät für Physik und Astronomie, Univ. Heidelberg, <https://doi.org/10.11588/heidok.00018209>, 2015.
- 30 Kräuter, C., Trofimova, D., Kiefhaber, D., Krah, N., and Jähne, B.: High resolution 2-D fluorescence imaging of the mass boundary layer thickness at free water surfaces, *J. Europ. Opt. Soc. Rap. Public.*, 9, 14016, <https://doi.org/10.2971/jeos.2014.14016>, 2014.
- Kunz, J. and Jähne, B.: Investigating small scale air-sea exchange processes via thermography, *Front. Mech. Eng.*, <https://doi.org/10.3389/fmech.2018.00004>, 2018.
- Lee, R. J. and Saylor, J. R.: The effect of a surfactant monolayer on oxygen transfer across an air/water interface during mixed convection, *Int. J. Heat Mass Transfer*, 53, 3405–3413, <https://doi.org/10.1016/j.ijheatmasstransfer.2010.03.037>, 2010.
- 35 Liss, P. S.: Processes of gas exchange across an air–water interface, *Deep-Sea Research*, 20, 221–238, [https://doi.org/10.1016/0011-7471\(73\)90013-2](https://doi.org/10.1016/0011-7471(73)90013-2), 1973.



- Liss, P. S. and Merlivat, L.: Air-sea gas exchange rates: Introduction and synthesis, in: *The Role of Air-Sea Exchange in Geochemical Cycling*, edited by Buat-Menard, P., pp. 113–129, Reidel, Boston, MA, https://doi.org/10.1007/978-94-009-4738-2_5, 1986.
- McKenna, S. P. and Bock, E. J.: Physicochemical effects of the marine microlayer on air-sea gas transport, in: *Marine Surface Films: Chemical Characteristics, Influence on Air-Sea Interactions, and Remote Sensing*, edited by Gade, M., Hühnerfuss, H., and Korenowski, G. M., pp. 77–91, Springer Berlin Heidelberg, https://doi.org/10.1007/3-540-33271-5_9, 2006.
- 5 McKenna, S. P. and McGillis, W. R.: The role of free-surface turbulence and surfactants in air-water gas transfer, *Int. J. Heat Mass Transfer*, 47, 539–553, <https://doi.org/10.1016/j.ijheatmasstransfer.2003.06.001>, 2004.
- Mesarchaki, E., Kräuter, C., Krall, K. E., Bopp, M., Helleis, F., Williams, J., and Jähne, B.: Measuring air–sea gas-exchange velocities in a large-scale annular wind–wave tank, *Ocean Sci.*, 11, 121–138, <https://doi.org/10.5194/os-11-121-2015>, 2015.
- 10 Nagel, L.: Active Thermography to Investigate Small-Scale Air-Water Transport Processes in the Laboratory and the Field, Dissertation, Institut für Umweltphysik, Fakultät für Chemie und Geowissenschaften, Univ. Heidelberg, <https://doi.org/10.11588/heidok.00016831>, 2014.
- Nagel, L., Krall, K. E., and Jähne, B.: Comparative heat and gas exchange measurements in the Heidelberg Aeolotron, a large annular wind-wave tank, *Ocean Sci.*, 11, 111–120, <https://doi.org/10.5194/os-11-111-2015>, 2015.
- 15 Nightingale, P. D., Malin, G., Law, C. S., Watson, A. J., Liss, P. S., Liddicoat, M. I., Boutin, J., and Upstill-Goddard, R. C.: In situ evaluation of air-sea gas exchange parameterization using novel conservation and volatile tracers, *Global Biogeochem. Cycles*, 14, 373–387, <https://doi.org/10.1029/1999GB900091>, 2000.
- Pereira, R., Schneider-Zapp, K., and Upstill-Goddard, R. C.: Surfactant control of gas transfer velocity along an offshore coastal transect: results from a laboratory gas exchange tank, *Biogeosciences*, 13, 3981–3989, <https://doi.org/10.5194/bg-13-3981-2016>, <https://www.biogeosciences.net/13/3981/2016/>, 2016.
- 20 Richter, K. and Jähne, B.: A laboratory study of the Schmidt number dependency of air-water gas transfer, in: *Gas Transfer at Water Surfaces 2010*, edited by Komori, S., McGillis, W., and Kurose, R., pp. 322–332, <https://doi.org/10.5281/zenodo.14955>, <http://hdl.handle.net/2433/156156>, 2011.
- Roether, W. and Kromer, B.: Optimum application of the radon deficit method to obtain air–sea gas exchange rates, in: *Gas transfer at water surfaces*, edited by Brutsaert, W. and Jirka, G. H., pp. 447–457, Reidel, Hingham, MA, https://doi.org/10.1007/978-94-017-1660-4_41, 1984.
- Sabbaghzadeh, B., Upstill-Goddard, R. C., Beale, R., Pereira, R., and Nightingale, P. D.: The Atlantic Ocean surface microlayer from 50N to 50S is ubiquitously enriched in surfactants at wind speeds up to 13 ms⁻¹, *Geophysical Research Letters*, 44, 2852–2858, <https://doi.org/10.1002/2017GL072988>, <http://dx.doi.org/10.1002/2017GL072988>, 2017GL072988, 2017.
- 30 Salter, M., Upstill-Goddard, R., Nightingale, P., Archer, S., Blomquist, B., Ho, D., Huebert, B., Schlosser, P., and Yang, M.: Impact of an artificial surfactant release on air-sea gas fluxes during Deep Ocean Gas Exchange Experiment II, *J. Geophys. Res.*, 116, C11016, <https://doi.org/10.1029/2011JC007023>, 2011.
- Schimpf, U., Nagel, L., and Jähne, B.: The 2009 SOPRAN active thermography pilot experiment in the Baltic Sea, in: *Gas Transfer at Water Surfaces 2010*, edited by Komori, S., McGillis, W., and Kurose, R., pp. 358–367, <https://doi.org/10.5281/zenodo.14956>, <http://hdl.handle.net/2433/156156>, 2011.
- 35 Schmidt, R.: Cruise Report of Alkor Cruise 336, <https://www2.bsh.de/akt/dat/dod/fahrtergebnis/2009/20100107.htm>, 2009.



- Schmidt, R. and Schneider, B.: The effect of surface films on the air–sea gas exchange in the Baltic Sea, *Marine Chemistry*, 126, 56 – 62, <https://doi.org/https://doi.org/10.1016/j.marchem.2011.03.007>, <http://www.sciencedirect.com/science/article/pii/S0304420311000375>, 2011.
- Schneider, B.: Cruise Report of Alkor Cruise 356, <https://www2.bsh.de/akt/dat/dod/fahrtergebnis/2010/20110109.htm>, 2010.
- 5 Toba, Y. and Koga, M.: A parameter describing overall conditions of wave breaking, whitecapping, sea-spray production, and wind stress, in: *Oceanic Whitecaps and Their Role in Air-Sea Exchange Processes*, pp. 37–47, D Reidel Pub Co, 1986.
- Wanninkhof, R.: Relationship between wind speed and gas exchange over the ocean, *J. Geophys. Res.*, 97, 7373–7382, <https://doi.org/10.1029/92JC00188>, 1992.
- Wanninkhof, R. and McGillis, W. R.: A cubic relationship between gas transfer and wind speed., *Geophys. Res. Lett.*, 26, 1889–1892, <https://doi.org/10.1029/1999GL900363>, 1999.
- 10 Woolf, D., Leifer, I., Nightingale, P., Rhee, T., Bowyer, P., Caulliez, G., de Leeuw, G., Larsen, S., Liddicoat, M., Baker, J., and Andreae, M.: Modelling of bubble-mediated gas transfer: Fundamental principles and a laboratory test, *J. Marine Syst.*, 66, 71–91, <https://doi.org/10.1016/j.jmarsys.2006.02.011>, 2007.
- Woolf, D. K.: Parametrization of gas transfer velocities and sea-state-dependent wave breaking, *Tellus B*, 57, 87–94, <https://doi.org/10.1111/j.1600-0889.2005.00139.x>, 2005.
- 15 Wurl, O., Wurl, E., Miller, L., Johnson, L., and Vagle, S.: Formation and global distribution of sea-surface microlayers, *Biogeosciences*, 8, 121–135, 2011.
- Zappa, C., Ho, D., McGillis, W., Banner, M., Dacey, J. W. H., Bliven, L., Ma, B., and Nystuen, J.: Rain-induced turbulence and air-sea gas transfer, *J. Geophys. Res.*, 114, C07 009, <https://doi.org/10.1029/2008JC005008>, 2009.
- 20 Zappa, C. J., Asher, W. E., Jessup, A. T., Klinke, J., and Long, S. R.: Microbreaking and the enhancement of air-water transfer velocity, *J. Geophys. Res.*, 109, C08S16, <https://doi.org/10.1029/2003JC001897>, 2004.
- Zhao, D., Toba, Y., Suzuki, Y., and Komori, S.: Effect of wind waves on air-sea gas exchange: proposal of an overall CO₂ transfer velocity formula as a function of breaking-wave parameter, *Tellus*, 55B, 478–487, <https://doi.org/10.1034/j.1600-0889.2003.00055.x>, 2003.